(Received 18 March 2025, Accepted 11 May 2025, Scheduled 14 May 2025)

Design and Optimization of Ultra-Wideband Dual-Notch Antenna Based on the BOLGB-DE Algorithm

Huawei Zhuang[1,*], Jianzhao Liu[1], Fangzhen Sun[1], Gaoqi Li[1], and Fanmin Kong[2]

[1] *School of Information & Electrical Engineering, Shandong Jianzhu University, Jinan 250101, China*
[2] *School of Information Science and Engineering, Shandong University, Tsingtao 266237, China*

ABSTRACT: With the rapid development of modern communication technologies, the use of ultra-wideband (UWB) notch antennas in various communication systems has increased significantly. However, designing UWB notch antennas with traditional methods often involves high complexity and low efficiency. To address the challenge, a novel optimization method, named BOLGB-DE (Bayesian optimization-Light Gradient Boosting Machine-Differential Evolution), is proposed. First, BOLGB model is selected as the surrogate model to establish the relationship between antenna design parameters and performance. Then, DE algorithm is used to invoke the BOLGB surrogate model to achieve the antenna optimization objectives. Compared to the traditional method, the BOLGB-DE method enables the reduction of electromagnetic simulations by 62% (from 1176 to 440 runs) and optimization time by 62% (from 22.8 hours to 8.6 hours). Finally, a UWB dual-notch antenna is designed using the BOLGB-DE method, featuring a dual-notch structure within the 1.9 GHz–10.1 GHz range. It achieves two notch bands (3.58 GHz–4.17 GHz for C-band downlink shielding and 5.12 GHz–5.38 GHz for 5G Wi-Fi interference suppression) while maintaining the target S_{11} values greater than -7 dB. The design requirements are successfully met by the antenna, as confirmed by the measurement results.

1. INTRODUCTION

With the rapid development of modern communication technologies, the use of ultra-wideband (UWB) antennas has become increasingly widespread. However, interference is caused between existing narrowband communication systems. To reduce interference, UWB notch antenna has been used increasingly [1, 2]. Due to the complex geometries of UWB notch antennas, the computational cost of antenna optimization is significantly high. Differential Evolution (DE) algorithm is selected for optimizing UWB notch antennas thanks to its superior global search capabilities [3]. When DE is used for high-dimensional optimization problems, more electromagnetic simulations are required, which increases costs and reduces efficiency, making it impractical [4–7].

Machine learning-based methods, including Gaussian process regression (GPR), support vector machine regression (SVR), neural networks (NN) [8], and others, are increasingly applied to solve multi-parameter antenna optimization problems [9–13]. These machine learning models, which can replace electromagnetic simulation software, are called surrogate models. By invoking surrogate model, the optimization process is accelerated, and the need for electromagnetic simulations is reduced [14, 15]. Extensive research has been conducted on surrogate modeling techniques for antenna optimization. AdaBoost algorithms demonstrated superior accuracy in electromagnetic modeling of multiband satellite antennas, achieving minimal errors in resonant frequency prediction compared to decision trees and random forests [16]. For polarization purity enhancement, a parallel surrogate model-assisted hybrid differential evolution for antenna synthesis (PSADEA)-optimized defected ground geometry reduced cross-polarization by 13–18 dB while maintaining 7.5–8.0 dBi gain, with tenfold acceleration over conventional methods [17]. In a miniaturized L-band antenna design, Bayesian-optimized neural networks enabled 92% volume reduction alongside 300% bandwidth expansion and 124% gain improvement [18]. Extreme randomized trees achieved exceptional accuracy for beam-steering prediction in graphene-based THz antennas, outperforming four other machine learning (ML) models in 6G network scenarios [19]. However, in practical optimization, a large number of training samples are typically required by these approaches, and the acquisition of samples and model training can be time-consuming with the efficiency benefits of the surrogate model being negated [20–25].

The S_{11} parameter curve of a UWB dual-notch antenna is characterized by two notch bands and multiple resonant points across the frequency ranges. Within these bands, dramatic variations in the S_{11} values challenge machine learning models [26]. The frequency points where the S_{11} value varies significantly are typically the focus of optimization efforts; therefore, prediction accuracy at these points directly affects optimization results. For UWB dual-notch antenna, the development of a highly accurate and cost-effective surrogate model is crucial.

Machine learning surrogate model methods are typically classified into online and offline approaches. The model is dynamically updated during optimization using the online method; however, local optima often occur due to uneven training data distribution, causing global solutions to be

* Corresponding author: Huawei Zhuang (zhuanghuawei@sdjzu.edu.cn).

overlooked. On the other hand, the model is trained only once using pre-generated sample data in the offline method. Therefore, in the offline method, high-quality samples are needed to train the model [27–29]. In the design of UWB dual-notch antennas, the optimization objectives are changed with the variation of the application scenarios. When the optimization objectives change, the surrogate model built by the online method cannot be reused and requires retraining and resampling. Therefore, the offline method is more suitable for the design of UWB dual-notch antennas. By conducting comprehensive sampling and constructing a surrogate model trained once, efficient optimization can be achieved within a clearly defined parameter range, and the model can be reused.

To address the inefficiency of the DE algorithm, the high training cost of machine learning surrogate models, and the complexity of predicting the performance of UWB dual-notch antennas, a novel approach, named BOLGB-DE (Bayesian optimization-Light Gradient Boosting Machine-Differential Evolution), is proposed. DE algorithm is combined with BOLGB surrogate model. Initially, the key parameters affecting the performance of UWB dual-notch antennas are identified through preliminary parameter scanning, and their optimization ranges are established. The parameter scanning process involves systematically adjusting various structural parameters of the antenna and analyzing their impact on key performance metrics, such as bandwidth and notch depth, among others. Specifically, if variations in a parameter result in a significant shift in the notch frequency or have a substantial impact on the antenna bandwidth, the parameter is considered a critical design factor. To ensure the surrogate model's generalization, a high-quality, uniformly distributed dataset is constructed using uniform sampling for key parameters. The Light Gradient Boosting Machine (LightGBM) model is trained on the dataset, with its hyperparameters adjusted through Bayesian optimization to ensure efficient training and high-precision predictions for the antenna dataset. Finally, BOLGB surrogate model is combined with DE algorithm to optimize antenna performance within the parameter range, with S_{11} values used as the objective function. It is confirmed by experimental results that the number of electromagnetic simulations and time costs are significantly reduced by the BOLGB-DE method, while the optimization objective is achieved.

The main innovations of this paper include:

1) Bayesian Optimization applied to the LightGBM model.

Bayesian optimization is applied to UWB dual-notch antenna design with LightGBM. The overfitting risk in datasets is reduced by adjusting LightGBM hyperparameters through Bayesian optimization. The histogram and leaf-wise algorithms, with depth limitations in LightGBM, are used to improve prediction accuracy at critical points with significant frequency variations. A high-precision surrogate model for antenna design optimization is created using the approach (validation can be found in Subsection 4.2).

2) The antenna optimization method based on BOLGB-DE is proposed.

The antenna parameters are optimized through iterative searches by the DE algorithm invoking the BOLGB surrogate model, thereby significantly reducing dependency on time-consuming electromagnetic simulations. Unlike direct evaluation of each candidate solution via full-wave simulations, the surrogate model is invoked to predict antenna performance efficiently, enabling DE to explore the design space more comprehensively and cost-effectively (validation details are provided in Subsection 4.3).

The remainder of this article is organized as follows. In Section 2, an overview of the antenna design and analysis is provided. In Section 3, the proposed BOLGB-DE algorithm is introduced, including data preparation, surrogate model construction and training, and the optimization of antenna parameters. In Section 4, the experimental studies are discussed, covering experimental parameter settings, validation of the surrogate model's prediction performance, and optimization results. Finally, in Section 5, the main contributions are summarized, and the prospects and significance of the research are discussed.

2. ANTENNA DESIGN AND ANALYSIS

In the design of UWB antennas, slotting techniques, parasitic elements, shorted lines, and defected ground structures (DGSs) are recognized as the methods for achieving dual-notch characteristics. Among them, slotting is a commonly used technique for notch design. By etching specific shapes of slots (such as C-shaped, L-shaped, U-shaped, and H-shaped slots) on the antenna's radiating patch, feedline, or ground plane, the surface current distribution of the antenna is altered, thereby creating the notch band at specific frequency ranges. Typically, the length of these slots is designed to be half or a quarter of the wavelength corresponding to the notch center frequency in order to achieve precise notch effects.

The UWB dual-notch antenna structure is shown in Fig. 1. The antenna is designed on an FR-4 substrate with a thickness of 1.6 mm, a relative permittivity of 4.4, and a loss tangent of 0.02. The substrate choice ensures a balance among cost, manufacturability, and electrical performance. The dual-notch characteristic of the antenna is primarily achieved through the slot structures on the front and rear sides of the antenna. The first notch is generated by a symmetric L-shaped slot etched on the front radiating patch, which alters the current path and introduces high impedance at specific frequency points, thereby creating the notch. The second notch is produced by a slot on the ground plane of the antenna. The structure adjusts the current distribution to effectively suppress signals in another specific frequency range.

Through preliminary parameter scanning, five key parameters and their optimization ranges are identified (units in mm): $L_{f1} \in [1, 3]$, $L_{f2} \in [8, 10]$, $L_{f3} \in [7.9, 8.4]$, $W_{f1} \in [4, 9]$, $W_{f2} \in [0.3, 0.4]$, which significantly influence the antenna's dual-notch characteristics and communication performance. The antenna's other structural parameters dimensions are presented in Table 1.

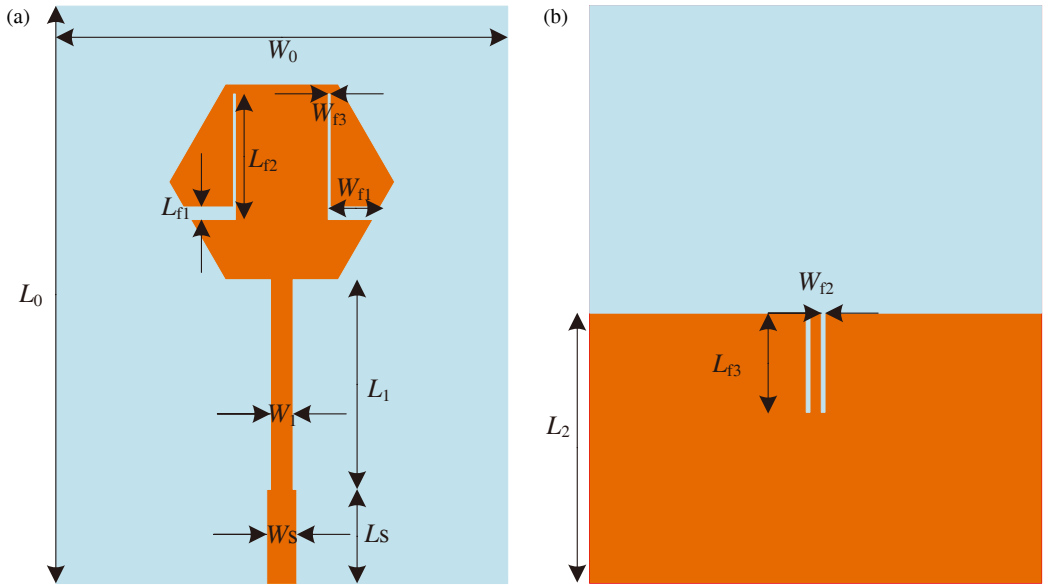

FIGURE 1. Antenna structure: (a) Front view of the antenna; (b) Back view of the antenna.

TABLE 1. Antenna structural parameters and dimensions.

Parameters	Dimensions (mm)
L_0	46.00
L_1	15.50
L_2	21.50
L_s	7.50
W_0	36.00
W_1	1.80
W_s	2.40

TABLE 2. Parameter sampling ranges and data points.

Eigen Value	Parameter Sampling Range
L_{f1}	(1.0 mm, 3.0 mm) step = 1.0 mm
L_{f2}	(8.0 mm, 10.0 mm) step = 1.0 mm
L_{f3}	(7.9 mm, 8.4 mm) step = 0.1 mm
W_{f1}	(4.0 mm, 9.0 mm) step = 1.0 mm
W_{f2}	(0.3 mm, 0.4 mm) step = 0.1 mm
F_{rep}	(0.5 GHz, 12.5 GHz) step = 0.1 GHz
Tag Value	**Number of Data Points**
S_{11}	53,240

3. PROPOSED BOLGB-DE ALGORITHM

BOLGB-DE algorithm is proposed for the efficient design and optimization of UWB dual-notch antennas. As shown in Fig. 2, the overall framework consists of four stages: data preparation, surrogate model construction and training, optimization of antenna parameters, and result validation.

3.1. Data Preparation

Based on the results of the parameter scanning, five parameters to be optimized and their optimization ranges are determined. A total of 440 sets of parameter combinations are generated by uniformly sampling within the ranges of the five key parameters at a specified step size. Each parameter combination is simulated using electromagnetic simulation software, and S_{11} values are obtained among 121 frequency points from 0.5 GHz to 12.5 GHz (with a step size of 0.1 GHz). The sampling steps and ranges (optimization ranges) are presented in Table 2.

The sampled data is used as the dataset, with 352 parameter combinations used for training, 44 for testing, and 44 for validation. The training set is used to train the BOLGB surrogate model, where the five structural parameters and frequency points are used as features, and the S_{11} value is used as the target. The validation set is used for early stopping during training, and the model's prediction performance is evaluated using the test set.

3.2. Surrogate Model Construction and Training

The BOLGB surrogate model constructed by Bayesian optimization of LightGBM hyperparameters is used as the prediction model to obtain the surrogate model $F(x)$, where x represents the five structural parameters and frequency points, and $F(x)$ corresponds to the S_{11} value of the antenna.

3.2.1. LightGBM for Surrogate Model Construction

LightGBM is an efficient machine learning algorithm based on Gradient Boosting Decision Trees (GBDTs), proposed by Microsoft Research Asia. The primary goal of LightGBM is to solve the efficiency bottleneck encountered by traditional GBDT when handling high-dimensional features and large-scale datasets. Its training process is shown in Fig. 3.

For a given dataset $T = \{(x_i, y_i)\}_{i=1}^{N}$, the objective is to find an approximate function $\hat{f}(x)$ that minimizes the expected loss function, as expressed in Equation ((1)):

$$\hat{f}(x) = \arg\min_{f} \mathbb{E}_{y\sim P(y|x)}[L(y, f(x))] \quad (1)$$

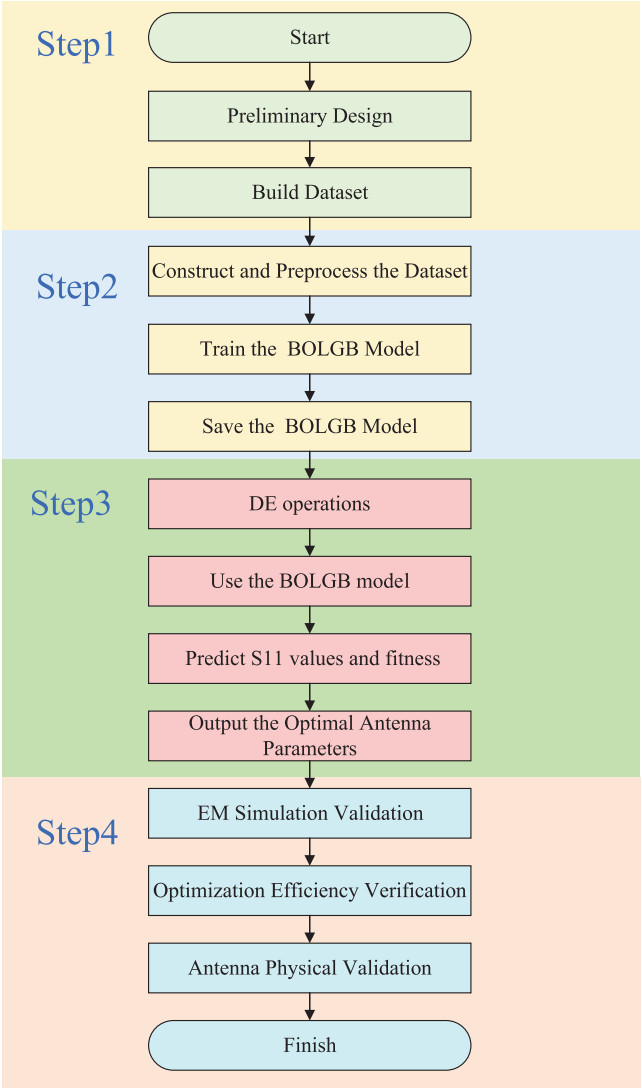

FIGURE 2. Overall framework of BOLGB-DE for antenna optimization.

In the equation, $L(y, f(x))$ represents the loss function that measures the discrepancy between the predicted value $f(x)$ and the true value y. The expectation $\mathbb{E}_{y\sim P(y|x)}$ is taken over the conditional distribution of y given x, denoted as $P(y|x)$. The goal is to find an optimal function $\hat{f}(x)$ that minimizes the expected loss.

Under the gradient boosting framework, the final model is approximated by an ensemble of m decision trees, denoted as $T_m(x)$. The model at the m-th iteration is formulated as shown in Equation ((2)):

$$f_m(x) = f_{m-1}(x) + T_m(x) \tag{2}$$

where $f_m(x)$ represents the model after m iterations, and $T_m(x)$ is the newly added decision tree. At each iteration, the model is iteratively refined by constructing a new tree to minimize the loss function.

As shown in Equation ((3)), the objective function at the k-th iteration is:

$$\Gamma_k = \sum_{i=1}^{N} L\left(y_i, f_k(x_i)\right) \tag{3}$$

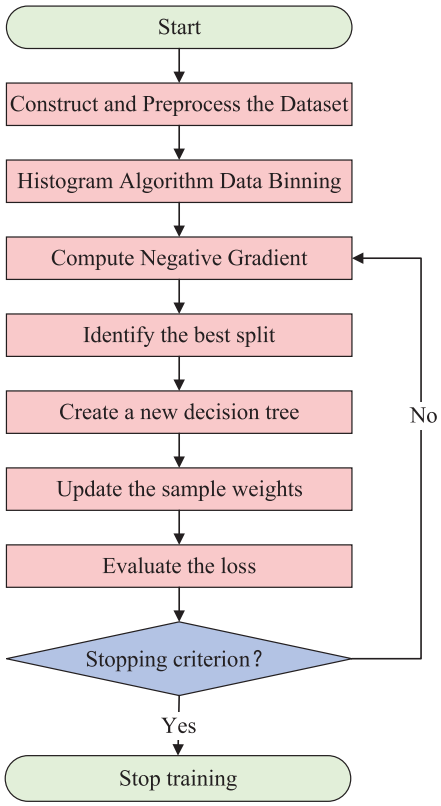

FIGURE 3. Training process of the LightGBM model.

After each iteration, the current loss value is computed by the LightGBM model, and a new decision tree is constructed to further minimize loss. Through the iterative process, LightGBM efficiently constructs multiple decision trees, continuously improving the model's performance.

Several optimization strategies are employed by the LightGBM algorithm, mainly including histogram optimization and the leaf-wise algorithm with depth limitation. Histogram optimization is shown in Fig. 4. The process of histogram optimization is constructed by discretizing continuous feature values into a limited number of integers. The process makes feature selection more efficient with memory usage reduced [30–33].

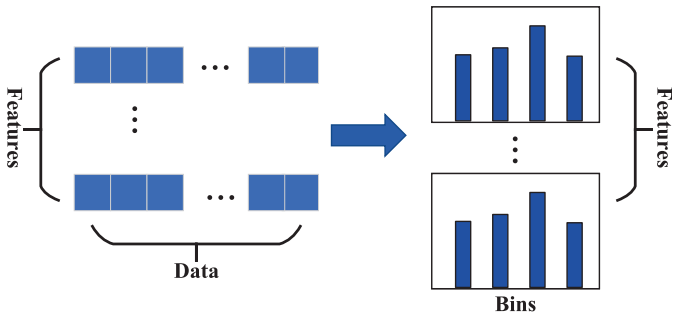

FIGURE 4. Process of histogram optimization.

Based on the histogram algorithm, further optimization is applied to LightGBM. The level-wise decision tree growth strategy, commonly used in most GBDT tools, is discarded, and the leaf-wise algorithm with depth limitation is adopted instead

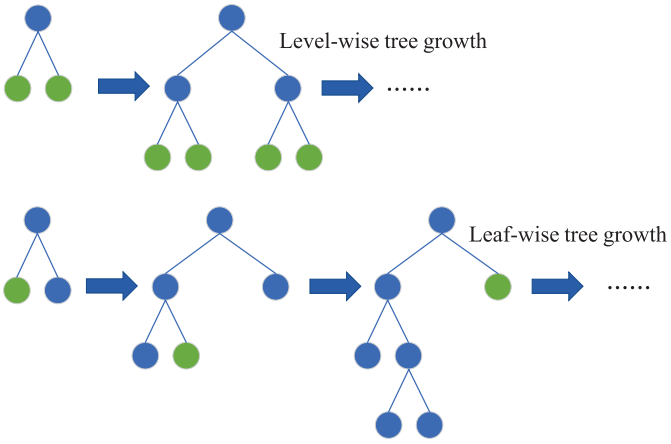

FIGURE 5. Comparison of level-wise and leaf-wise splitting methods.

[34]. The level-wise and leaf-wise splitting methods are shown in Fig. 5. In the leaf-wise strategy, the leaf with the highest splitting gain is selected at each step, split, and the process is repeated. Compared to the level-wise approach, the advantages of the leaf-wise strategy are as follows: for the same number of splits, more error is reduced, and better accuracy is achieved with the leaf-wise strategy. However, its disadvantage is that deeper decision trees may be generated, which can lead to overfitting. Therefore, a maximum depth limitation is introduced based on the leaf-wise strategy in LightGBM to prevent overfitting while maintaining high efficiency.

3.2.2. Bayesian Hyperparameter Optimization for LightGBM

Bayesian optimization is an efficient method for optimizing black-box functions and is particularly suited for high-dimensional and computationally expensive objective function problems. The core principle of the method is based on the approximation of the objective function using a surrogate model, and the next sampling point is determined through an acquisition function, allowing the global optimal solution to be iteratively refined [35–37]. In the Bayesian optimization of hyperparameters, the GPR model is typically employed to construct a surrogate function, where different hyperparameter sets are mapped to their corresponding error metrics on the validation set. The objective function is approximated through the development of a flexible surrogate model. A key advantage of the Gaussian process is that both the predicted mean of function values and the associated uncertainty are provided, which is considered as a crucial factor for Bayesian optimization.

In the context of LightGBM, hyperparameters such as maximum number of leaves (integer range from 20 to 50), learning rate (real values between 0.01 and 0.1, using a log-uniform prior), feature fraction (real values between 0.7 and 1.0, using a uniform prior), and number of estimators (integer range from 50 to 300) are optimized to improve model performance. The combination of Bayesian optimization's ability to model uncertainty and LightGBM's efficiency in handling datasets and high-dimensional features provides a powerful approach for tackling complex machine learning tasks. The synergy enhances model performance by identifying the most promising hyperparameter configurations while reducing the risk of overfitting.

3.3. Optimization of Antenna Parameters

The BOLGB surrogate model is invoked by the DE algorithm to obtain the S_{11} values at the needed frequency points, which are then used to calculate the fitness function. Through iterations, the algorithm gradually approaches the target values and obtains the optimal antenna parameters, completing the optimization process. The antenna design parameters are optimized by considering multiple performance metrics. There are two optimization objectives.

The first objective of the antenna is for the dual-notch characteristics to be achieved in band1 (3.6 GHz to 4.2 GHz, 5.1 GHz to 5.4 GHz) within the 0.5 GHz to 12.5 GHz frequency range.

Optimization Objective 1:

$$\begin{cases} \underset{freq\in \text{band 1}}{S_{11}} > -7\text{dB} \\ \underset{freq\notin \text{band 1}}{Minimize\, S_{11}} \end{cases} \tag{4}$$

It is worth noting that, although an S_{11} value greater than -10 dB is theoretically considered sufficient to achieve notch functionality, antennas with an S_{11} value of -10 dB are still capable of functioning in practical applications. For improved notch performance, the optimization target has been set to require the S_{11} value of the specified frequency bands to be greater than -7 dB.

In order to ensure optimal communication performance during operation, the second optimization objective of the antenna is to ensure that the S_{11} values in band2 (2.7 GHz to 3.1 GHz, 5.7 GHz to 6.1 GHz, and 4.3 GHz to 4.7 GHz) are maintained below -15 dB.

Optimization Objective 2:

$$\underset{freq\in \text{band 2}}{S_{11}} < -15\,\text{dB} \tag{5}$$

In the DE algorithm, the optimization objective is set to maximize the total score. The total score is composed of two main components: the Optimization Objective 1 score, named $score_1$, and the Optimization Objective 2 score, named $score_2$. These two scores are combined through a weighted sum to form the total score, which is used to evaluate the overall performance of the design parameters.

To achieve Optimization Objective 1, the scoring rule is given by Equation ((6)). For the dual-notch frequency bands, target band1 (3.6 GHz to 4.2 GHz and 5.1 GHz to 5.4 GHz), frequencies with S_{11} values greater than -7 dB are rewarded. For non-target notch bands within the 0.5 GHz to 12.5 GHz range, excluding the target notch bands, high S_{11} values are penalized using a penalty factor, denoted as $factor_1$. Frequencies within notch band1 with S_{11} values not greater than -7 dB are also penalized to ensure that good notch performance is exhibited only within the target notch bands, while S_{11} values in other frequency bands are minimized to maintain good communica-

tion performance.

$$penalty_1 = factor_1 \times \left(\sum_{\substack{S_{11}>-7 \\ freq \notin \text{band 1}}} (S_{11}+7) + \sum_{\substack{S_{11}<-7 \\ freq \in \text{band 1}}} (-S_{11}-7) \right) \quad (6)$$

$$score_1 = \sum_{\substack{S_{11}>-7 \\ freq \in \text{band1}}} (S_{11}+7) - penalty_1$$

The scoring rule for Optimization Objective 2 is given by Equation (7). Objective 2 primarily aims to further improve the antenna's performance in the operating frequency bands, specifically in the following bands: band 2 (2.7 GHz to 3.1 GHz, 5.7 GHz to 6.1 GHz, and 4.3 GHz to 4.7 GHz). When the S_{11} value in band2 is below -15 dB, the antenna is considered to exhibit good communication performance at these frequencies, and scores are assigned to those frequency points.

$$score_2 = \sum_{\substack{S_{11}<-15 \\ freq \in \text{band2}}} (-15 - S_{11}) \quad (7)$$

Different weights are assigned to Objective 1 and Objective 2, denoted by α and β, and the $Total\ score$ is obtained through weighted summation, which is calculated as shown in Equation ((8)):

$$Total\ score = \alpha \cdot score_1 + \beta \cdot score_2 \quad (8)$$

The optimization process begins with the initialization of a population of candidate solutions, where each solution represents a set of antenna parameters. These initial solutions are randomly generated within the defined search space. For each candidate solution, the fitness function is evaluated by invoking the BOLGB surrogate model to obtain the corresponding S_{11} values at the specified frequency points, which are then used to calculate the $Total\ score$. Next, the DE algorithm performs mutation, generating new candidate solutions by combining individuals from the current population. This is followed by the crossover operation, where the mutated solutions and original solutions are combined to create new candidate solutions. After mutation and crossover, the selection process determines which individuals will survive to the next generation. The $Total\ score$ of each candidate solution is compared, and solutions with higher total scores are retained. The optimization process continues iteratively, with the population evolving toward the optimal solution. The algorithm terminates once the stopping criteria are met, such as reaching a maximum number of generations or achieving $Target\ score$.

Ultimately, the DE algorithm identifies the best antenna design parameters that maximize the $Total\ score$, thus achieving the optimization objective. After the optimal parameters are obtained, full-wave electromagnetic simulations are performed to verify the optimization results and efficiency analysis. The antenna is then fabricated for physical testing.

4. EXPERIMENTAL STUDIES

The optimization results and analysis of the UWB dual-notch antenna model are presented using the proposed BOLGB-DE algorithm in the section. The experimental parameter setup is described in Subsection 4.1. The prediction performance of the BOLGB surrogate model is verified in Subsection 4.2 by comparing its error metrics and training time with those of other machine learning models. In Subsection 4.3, the results of the antenna optimization are analyzed. The effectiveness of the proposed method is validated through comparisons with other optimization methods and through the fabrication of the optimized antenna for physical testing.

4.1. Experimental Parameter Settings

As shown in Equation (8), the $Total\ score$ is obtained through weighted summation, where different weights α and β are assigned to Objective 1 and Objective 2. Multiple experimental comparisons have shown that setting $\alpha = 0.8$ and $\beta = 0.2$ most effectively balances the two optimization objectives. The best performance of the antenna in the notch band is ensured by the weight combination, while the optimization of the operating frequency band is also considered, thereby, good performance in various application scenarios is ensured.

In order to reduce the computational costs and ensure the effectiveness of the optimization results, the $Target\ score$ is set based on preliminary simulations and empirical test results. The impacts of different $Target\ scores$ on optimization performance are compared in multiple experiments. It is found that when the $Total\ score$ reaches 25, the optimization goal is achieved while effectively avoiding excessive iterations and high computational costs. Therefore, the $Target\ score$ of 25 is chosen as a balance point for the optimization, ensuring both optimization performance and control of computational resources. Thus, the stopping condition for the DE algorithm is set to reach either the $Target\ score$ of 25 or the maximum number of iterations.

4.2. Performance Validation of the BOLGB Surrogate Model

The performance of the BOLGB surrogate model is validated by comparing the predictive performances of seven different machine learning models. All models are trained using the same training and test datasets, with hyperparameters tuned through Bayesian optimization. The seven comparison models are SVR, eXtreme Gradient Boosting (XGBoost), Stochastic Gradient Descent (SGD), K-Nearest Neighbors (KNNs), Ridge Regression (Ridge), Decision Tree (DT), and Gradient Boosting (GB).

Mean Squared Error (MSE), Root Mean Squared Error (RMSE), Mean Absolute Error (MAE), Coefficient of Determination (R^2) are included in the main evaluation metrics. The performance comparison results are presented in Table 3, with R^2 being used to measure the model's fit to the data. A bar chart comparing the R^2 values of each model is shown in Fig. 6, with differences in their fitting capabilities highlighted.

The BOLGB surrogate model's best prediction performance is shown in Fig. 6 and Table 3, while models such as GB and

TABLE 3. Comparison of models' predicted performance across all frequency points based on key metrics.

Algorithms	MSE	RMSE	MAE	R^2	Training Time
Bayesian-SVR	18.54	4.31	2.96	0.48	36264 s
Bayesian-XGBoost	5.55	2.36	1.48	0.84	81.44 s
Bayesian-SGD	35.38	5.95	4.91	0.01	37.98 s
Bayesian-KNN	4.32	2.08	1.05	0.87	52.24 s
Bayesian-Ridge	35.38	5.95	4.91	0.01	25.32 s
Bayesian-DT	3.26	1.80	1.44	0.90	34.15 s
Bayesian-GB	2.94	1.72	1.38	0.91	397.67 s
BOLGB	2.33	1.53	0.82	0.94	70.57 s

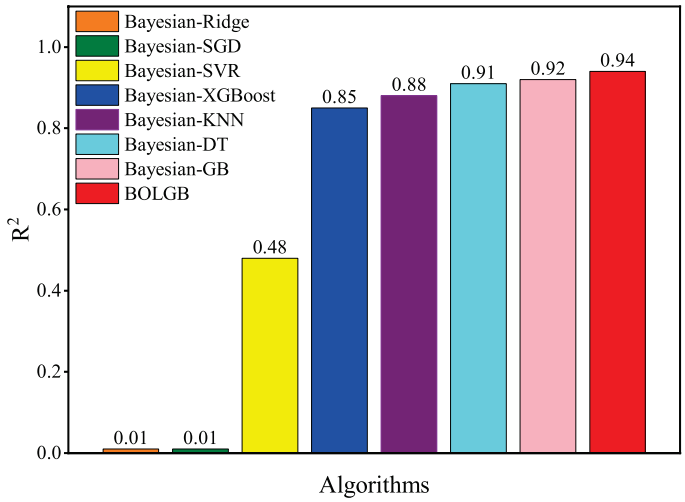

FIGURE 6. Comparison of models' predicted performances across all frequency points based on R^2 values.

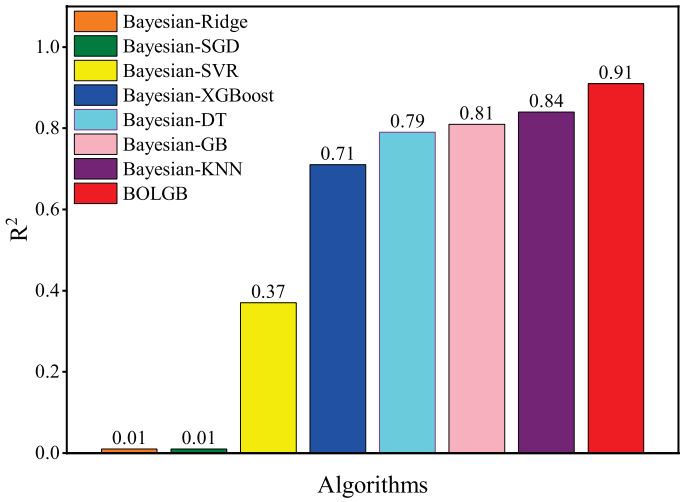

FIGURE 7. Comparison of models' predicted performances at notch frequency points based on R^2 values.

DT also perform well. However, only the overall prediction capability of the test set samples in the 0.5 GHz to 12.5 GHz range is reflected by these results. Relying solely on this data is not considered sufficient to fully demonstrate the prediction capability of the model. This is because the accurate prediction of the S_{11} values in the notch bands and certain resonance points is deemed crucial when the surrogate model is used to optimize the notch antenna. These bands are typically targeted for optimization, and prediction errors in these regions are likely to significantly impact the optimization results. Therefore, better optimization results can only be achieved if high prediction accuracy is maintained in these critical regions during the subsequent optimization process.

A total of 44 antenna samples with different sizes are included in the test set, 24 of which are found to exhibit dual-notch characteristics in different frequency bands. To ensure that the advantages of the BOLGB surrogate model in predicting the S_{11} values in frequency bands with significant variations are more comprehensively validated, 24 samples that meet the dual-notch criteria are selected. For these samples, 10 frequency points within the notch bands are evenly sampled, resulting in 240 data points. These data points are then predicted using the eight models mentioned above, and the prediction performance of each model is evaluated by comparing their R^2. The prediction results of the models are shown in Fig. 7.

A more intuitive comparison of the model's predictive performance is provided by selecting a representative sample from the test set. The sample exhibits two notches and multiple resonance points, making it a suitable case for evaluation. The parameters are as follows: $L_{f1} = 1\,\text{mm}$, $L_{f2} = 8\,\text{mm}$, $L_{f3} = 7.9\,\text{mm}$, $W_{f1} = 5\,\text{mm}$, and $W_{f2} = 0.4\,\text{mm}$. The scatter plot comparison of the predicted S_{11} values and simulated values for this sample under the eight models is shown in Fig. 8.

By analyzing the above results, it is found that the BOLGB surrogate model is consistently shown to have the best prediction performance among all models, both in the overall frequency band and in the frequency bands with significant changes in S_{11} values. In contrast, poor performance is observed in the SVR, Ridge, and SGD models for predicting S_{11} values of the antenna. This is primarily due to the inability of these models to effectively capture the complex nonlinear relationships in the data, rendering them unsuitable for predicting the S_{11} values of dual-notch antennas. It is observed that the DT, GB, KNN, and XGBoost models perform well on the overall data in the 0.5 GHz to 12.5 GHz range. However, as shown in Fig. 7, a significant decrease in prediction accuracy is seen

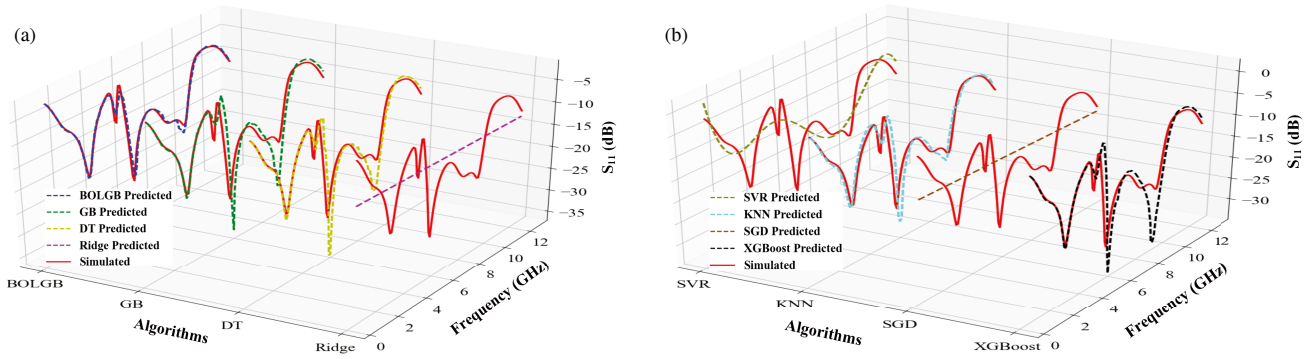

FIGURE 8. Scatter plot comparison of predicted and simulated S_{11} values for different models: (a) BOLGB, GB, DT, and Ridge models; (b) SVR, KNN, SGD, and XGBoost models.

in the notch frequency bands. The decline in prediction accuracy at frequency bands with significant changes in S_{11} values is more clearly illustrated in the test set sample shown in Fig. 8. The fitting ability of these models at frequency points with dramatic changes in S_{11} values (such as 6 GHz, 9 GHz, and the notch points) is notably inferior to that of the BOLGB surrogate model.

The superior performance of the BOLGB surrogate model over other models is attributed to the unique leaf-wise tree growth strategy and histogram-based decision tree algorithm of the LightGBM model. At the same time, the Bayesian optimization algorithm for hyperparameter tuning, can provide higher flexibility and accuracy in handling complex nonlinear relationships. Through the verification of the above experimental results, it has been demonstrated that the BOLGB surrogate model excels in predicting the S_{11} values of UWB dual-notch antennas, especially at key frequency points where S_{11} values change drastically. It can thus be used as a surrogate model for the subsequent DE optimization algorithm.

4.3. Validation of BOLGB-DE Optimization Results

Six optimizations are performed using BOLGB-DE to eliminate random factors, and the optimization objective is achieved in all six cases. The S_{11} results from the six optimizations are presented in Fig. 9, and the six best parameters from these optimizations are listed in Table 4.

Note: To enhance the visualization of the optimization results in the notch frequency bands, four vertical dashed lines at the x-axis, corresponding to 3.6 GHz, 4.2 GHz, 5.1 GHz, and 5.4 GHz, are shown in Fig. 9 and Fig. 11.

Antenna sample 1 is selected as the final optimization result, and its performance is specifically validated below. Two excellent notch bands are featured with S_{11} values greater than -7 dB. These notch bands can be used to shield the extended C-band downlink communication (3.625 GHz to 4.2 GHz) and the 5G Wi-Fi frequency band (5.15 GHz to 5.35 GHz).

The radiation patterns of antenna sample 1 at two frequency points (2.9 GHz and 5.9 GHz) are shown in Fig. 10. At these two frequency points, the E-plane radiation patterns exhibit an 8-shaped pattern, while omnidirectional radiation is observed in the H-plane. This indicates that directive radiation is exhibited

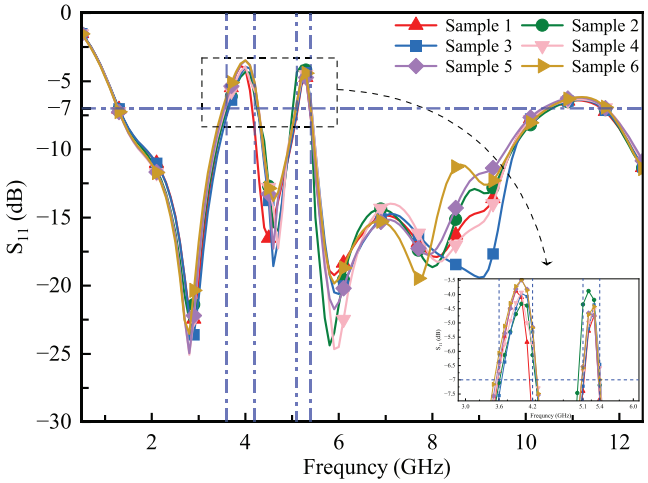

FIGURE 9. S_{11} simulated results of 6 optimized parameters using BOLGB-DE.

in the E-plane and omnidirectional radiation in the H-plane. Furthermore, at these frequency points, the cross-polarization component gains are significantly lower than those of the main polarization components, indicating that high polarization purity is achieved, and cross-polarization interference is minimized. It is suitable for antenna applications to require efficient signal transmission and minimized interference.

To comprehensively validate the effectiveness of machine learning-based surrogate models in optimization accuracy and efficiency, six methods are compared: BOLGB-DE, EM-DE (direct electromagnetic simulation-driven DE), and four surrogate-assisted models (KNN-DE, GB-DE, DT-DE, XGBoost-DE). Six independent optimization runs are conducted under identical parameter configurations. As summarized in Table 5, the evaluation metrics included model construction time (T1, comprising dataset preparation t1 and model training t2), optimization time T2, total computational time, simulation runs, and success counts (defined as achievement of optimization targets).

The BOLGB-DE method demonstrated 100% success rate (6/6), significantly outperforming XGBoost-DE (3/6) and DT-DE (4/6). The superior performance is attributed to its enhanced prediction accuracy and optimization stability. Regard-

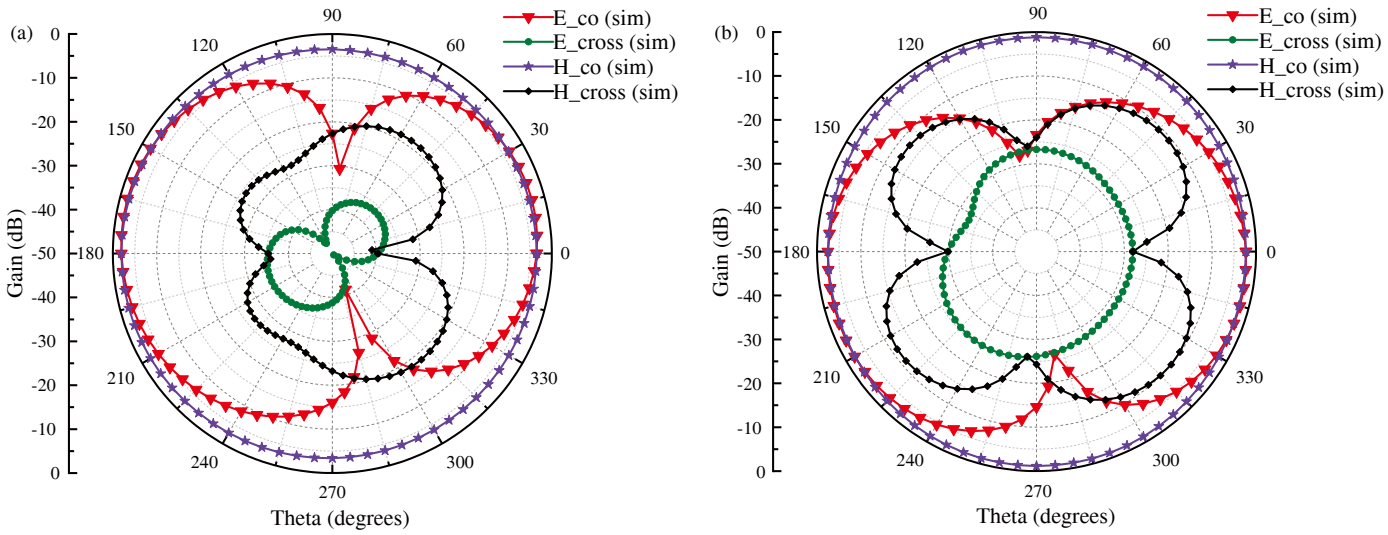

FIGURE 10. Simulated radiation patterns at frequencies of (a) 2.9 GHz and (b) 5.9 GHz.

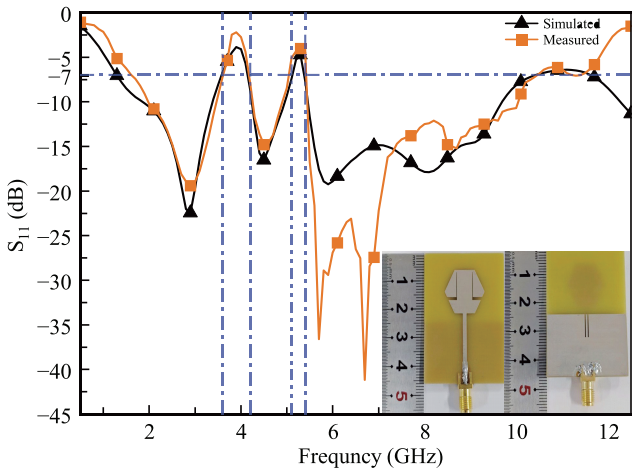

FIGURE 11. Measured and simulated results of antenna sample 1, along with the physical image of the antenna.

ing computational efficiency, all machine learning-based methods (BOLGB-DE: 8.64 hours, KNN-DE: 8.73 hours, GB-DE: 8.68 hours) showed comparable total times that are substantially lower than the EM-DE model (22.8 hours). The BOLGB-DE method achieved a 62% reduction in simulation runs, requiring only 440 electromagnetic simulations (69.9 seconds per simulation) compared to 1176 simulations for EM-DE. It is contributed to the observed time savings. Notably, while KNN-DE and GB-DE achieved similar computational durations (8.64–8.73 hours), their lower success rates (5/6 and 4/6, respectively) highlighted the critical importance of surrogate model precision in avoiding local optima. These results confirm that BOLGB-DE provides an optimal balance between computational efficiency (8.54 hours for dataset generation and 70.57 seconds for model training) and optimization reliability, establishing it as a high-precision design tool for UWB dual-notch antennas.

It is important to note that the advantage of an offline dataset is that when our design goals change, such as changes in the target notch bands, the previously trained model can still be reused. However, the re-parameter search is required when the dataset is updated online. Therefore, the optimization efficiency is significantly improved by the establishment of an offline surrogate model when different design requirements arise.

To comprehensively validate the effectiveness of this design, antenna sample 1 was fabricated. Fig. 11 shows the measured and simulated results of antenna sample 1, along with the physical image of the antenna.

The physical testing is conducted to validate the effectiveness of the BOLGB-DE optimization method. The physical measurement results of the antenna showed that the antenna featured a dual-notch design within the 1.9 GHz–10.1 GHz range, with two notch bands at 3.58 GHz–4.17 GHz and 5.12 GHz–5.38 GHz. In comparison, the simulated results indicated that the antenna featured a dual-notch design within the 1.29 GHz–10.42 GHz range, with notch bands at 3.57 GHz–4.15 GHz and 5.13 GHz–5.37 GHz. Although there are some differences between the simulated and measured results in certain frequency bands, the overall trend remains consistent. The antenna achieves the expected notch characteristics and meets the operational requirements of the working frequency band.

According to the experimental results, it is confirmed that the proposed BOLGB algorithm not only achieves high-precision prediction of the antenna S_{11} parameter but also accomplishes the optimization objectives with a 62% reduction in simulation runs compared to conventional methods. The superior dual-notch performance is further validated through measurements conducted on the fabricated antenna. Compared to the KNN algorithm [38], XGBoost algorithm [39], and GB algorithm [40], the improvement is primarily attributed to the optimization of the histogram-based algorithm and the depth-constrained Leaf-wise tree growth strategy adopted in the LightGBM framework. In addition, the hyperparameter of the surrogate model is optimized via the Bayesian optimization algorithm, resulting in a significant enhancement in prediction accuracy. Finally, the strong global search capability of the DE algorithm is used to efficiently achieve the optimization objectives.

TABLE 4. Six parameter sets from 6 optimizations using BOLGB-DE.

Parameters (mm)	Sample 1	Sample 2	Sample 3	Sample 4	Sample 5	Sample 6
L_{f1}	1.00	1.00	1.00	1.00	1.37	1.28
L_{f2}	10.00	8.84	9.95	8.88	10.00	9.43
L_{f3}	8.00	7.98	7.90	8.07	8.05	7.90
W_{f1}	4.21	5.02	4.84	4.76	4.53	4.84
W_{f2}	0.34	0.40	0.40	0.40	0.37	0.40

TABLE 5. Comparison of efficiency between BOLGB-DE and EM-DE.

Methods	T1	T2	Overall Time	Simulation Runs	Success Counts
BOLGB-DE	30826 s	282 s	8.64 h	440	6
EM-DE	-	22.8 h	22.8 h	1176	6
KNN-DE	30808 s	296 s	8.64 h	440	5
GB-DE	31153 s	279 s	8.73 h	440	5
DT-DE	30790 s	370 s	8.69 h	440	4
XGBoost-DE	30837 s	459 s	8.6 h	440	3

5. CONCLUSION

A novel optimization method, BOLGB-DE, is presented, which combines the Bayesian optimization of hyperparameters in LightGBM with DE algorithm. The proposed method enables the efficient design and optimization of UWB dual-notch antennas. Through a comparative analysis of various machine learning models, the advantages of the BOLGB-DE algorithm in improving optimization efficiency and prediction accuracy are validated. During the optimization process, the number of electromagnetic simulations is significantly reduced by the BOLGB-DE algorithm, and the optimization results are validated through experiments. Finally, physical fabrication and testing of the antenna sample with the best optimized parameters further confirmed the accuracy of the design and the predictive performance of the model. It is demonstrated that the BOLGB-DE method exhibits broad application potential in electromagnetic design. Future applications could be extended to multi-band antennas, reconfigurable antennas, miniaturized wearable devices, phased array systems, and microwave component design. By significantly reducing computational costs and efficiently addressing complex optimization problems, the proposed method is regarded as an ideal tool for high-performance antenna design and optimization.

ACKNOWLEDGEMENT

This work was supported by the Natural Science Foundation of Shandong (ZR2021QD066).

REFERENCES

[1] Alazemi, A. J. and Y. T. Alsaleh, "An ultrawideband antenna with two independently tunable notch bands," *Alexandria Engineering Journal*, Vol. 79, 402–410, 2023.

[2] Platt, J. M., L. B. Boskovic, and D. S. Filipovic, "Wideband biconical antenna with embedded band-notch resonator," *IEEE Transactions on Antennas and Propagation*, Vol. 72, No. 3, 2921–2925, 2024.

[3] Akhitha, K. and G. Ram, "Side lobe reduction and interference rejection in concentric hexagonal antenna array using differential evolutionary algorithm," in *2022 IEEE Microwaves, Antennas, and Propagation Conference (MAPCON)*, 681–685, Bangalore, India, 2022.

[4] Storn, R. and K. Price, "Differential evolution — A simple and efficient heuristic for global optimization over continuous spaces," *Journal of Global Optimization*, Vol. 11, 341–359, Dec. 1997.

[5] Liu, Y., B. Liu, M. Ur-Rehman, M. A. Imran, M. O. Akinsolu, P. Excell, and Q. Hua, "An efficient method for antenna design based on a self-adaptive bayesian neural network-assisted global optimization technique," *IEEE Transactions on Antennas and Propagation*, Vol. 70, No. 12, 11 375–11 388, Dec. 2022.

[6] Ye, F., Z. You, D. Zhang, and S. C. H. Leung, "Discrete differential evolutionary algorithm for job-shop scheduling problem with minimizing total weighted tardiness," in *2016 IEEE Congress on Evolutionary Computation (CEC)*, 56–62, Vancouver, BC, Canada, 2016.

[7] Xia, S., M. Li, and J. Yu, "Logistics transportation system based on the differential evolutionary algorithm," in *2020 Chinese Automation Congress (CAC)*, 5817–5820, Shanghai, China, 2020.

[8] Aneesh, M., J. A. Ansari, A. Singh, S. Verma, *et al.*, "RBF neural network modeling of rectangular microstrip patch antenna," in *2012 Third International Conference on Computer and Communication Technology*, 241–244, Allahabad, India, Nov. 2012.

[9] Chen, W., Q. Wu, C. Yu, H. Wang, and W. Hong, "Multibranch machine learning-assisted optimization and its application to antenna design," *IEEE Transactions on Antennas and Propagation*, Vol. 70, No. 7, 4985–4996, 2022.

[10] Kan, D., D. Spina, S. D. Ridder, F. Grassi, H. Rogier, and D. V. Ginste, "A machine-learning-based epistemic modeling framework for textile antenna design," *IEEE Antennas and Wireless Propagation Letters*, Vol. 18, No. 11, 2292–2296, 2019.

[11] Shi, L. P., Q. H. Zhang, S. H. Zhang, G. X. Liu, and C. Yi, "Predicting electromagnetic response of graphene reconfigurable patch antenna using SVR," in *2020 IEEE International Conference on Computational Electromagnetics (ICCEM)*, 34–36, Singapore, 2020.

[12] Zhang, J., M. O. Akinsolu, B. Liu, and S. Zhang, "Design of zero clearance SIW endfire antenna array using machine learning-assisted optimization," *IEEE Transactions on Antennas and Propagation*, Vol. 70, No. 5, 3858–3863, 2022.

[13] Sharma, Y., H. H. Zhang, and H. Xin, "Machine learning techniques for optimizing design of double T-shaped monopole antenna," *IEEE Transactions on Antennas and Propagation*, Vol. 68, No. 7, 5658–5663, Jul. 2020.

[14] Han, K.-H. and J.-H. Kim, "Quantum-inspired evolutionary algorithm for a class of combinatorial optimization," *IEEE Transactions on Evolutionary Computation*, Vol. 6, No. 6, 580–593, Dec. 2002.

[15] Schulz, E., M. Speekenbrink, and A. Krause, "A tutorial on Gaussian process regression: Modelling, exploring, and exploiting functions," *Journal of Mathematical Psychology*, Vol. 85, 1–16, Aug. 2018.

[16] Kumar, A., T. Khan, and D. Sarkar, "Forward-inverse-hybrid modeling of microstrip antennas using decision tree-based machine learning algorithms for space communication," *AEU — International Journal of Electronics and Communications*, Vol. 191, 155662, 2025.

[17] Rafidul, S., M. O. Akinsolu, B. Liu, C. Kumar, and D. Guha, "Machine learning-assisted microstrip antenna design featuring extraordinary polarization purity," *IEEE Antennas and Wireless Propagation Letters*, Vol. 24, No. 4, 1008–1012, 2025.

[18] Chatterjee, D. and A. K. Kundu, "Design and optimization of a meander line radiator inspired miniaturized microstrip patch antenna using machine learning," *MAPAN*, 1–26, 2025.

[19] Fakharian, M. M., "Machine learning approach for evaluation of beam-string in a metasurface-based terahertz antenna for 6G networks," *Materials Today Communications*, Vol. 43, 111671, 2025.

[20] Shakya, S. R., M. Kube, and Z. Zhou, "A comparative analysis of machine learning approach for optimizing antenna design," *International Journal of Microwave and Wireless Technologies*, Vol. 16, No. 3, 487–497, 2024.

[21] Babale, S. A., T. K. Geok, S. K. A. Rahim, C. P. Liew, U. Musa, M. F. Hamza, Y. A. Bakhuraisa, and L. L. Lim, "Machine learning-based optimized 3G/LTE/5G planar wideband antenna with tri-bands filtering notches," *IEEE Access*, Vol. 12, 80 669–80 686, 2024.

[22] Zhang, J., J. Xu, Q. Chen, and H. Li, "Machine-learning-assisted antenna optimization with data augmentation," *IEEE Antennas and Wireless Propagation Letters*, Vol. 22, No. 8, 1932–1936, 2023.

[23] Prado, D. R., J. A. López-Fernández, M. Arrebola, and G. Goussetis, "Support vector regression to accelerate design and crosspolar optimization of shaped-beam reflectarray antennas for space applications," *IEEE Transactions on Antennas and Propagation*, Vol. 67, No. 3, 1659–1668, Mar. 2019.

[24] Zhu, S.-H., X.-S. Yang, J. Wang, and B.-Z. Wang, "Design of MIMO antenna isolation structure based on a hybrid topology optimization method," *IEEE Transactions on Antennas and Propagation*, Vol. 67, No. 10, 6298–6307, Oct. 2019.

[25] Koziel, S. and S. Ogurtsov, "Multi-objective design of antennas using variable-fidelity simulations and surrogate models," *IEEE Transactions on Antennas and Propagation*, Vol. 61, No. 12, 5931–5939, Dec. 2013.

[26] Rizvi, S. N. R., W. A. Awan, D. Choi, N. Hussain, S. G. Park, and N. Kim, "A compact size antenna for extended UWB with WLAN notch band stub," *Applied Sciences*, Vol. 13, No. 7, 4271, 2023.

[27] Ustun, D., M. Tekbas, and A. Toktas, "Determination of feed point by surrogate model based on radial basis function for rectangular microstrip antennas," in *2019 International Artificial Intelligence and Data Processing Symposium (IDAP)*, 1–3, Malatya, Turkey, Sep. 2019.

[28] Shi, D., C. Lian, K. Cui, Y. Chen, and X. Liu, "An intelligent antenna synthesis method based on machine learning," *IEEE Transactions on Antennas and Propagation*, Vol. 70, No. 7, 4965–4976, 2022.

[29] Peng, F. and X. Chen, "Quantum-inspired algorithm enhances efficiency in antenna optimization," *IEEE Transactions on Antennas and Propagation*, Vol. 72, No. 9, 6980–6991, Sep. 2024.

[30] Qi, C., Y. Liu, Y. Wang, and M. Dong, "A classification method for electricity users based on the LightGBM algorithm," in *2023 IEEE 7th Conference on Energy Internet and Energy System Integration (EI2)*, 4815–4819, Hangzhou, China, 2023.

[31] Meng, F. and H. Zhou, "Iterative LightGBM algorithm and application on difficulty modeling of chinese reading materials in middle school based on psychological feature extraction," in *2022 IEEE 4th Eurasia Conference on IOT, Communication and Engineering (ECICE)*, 332–335, Yunlin, Taiwan, 2022.

[32] Fan, M., Y. Liu, X. Zhang, H. Chen, Y. Hu, L. Fan, and Q. Yang, "Fault prediction for distribution network based on CNN and LightGBM algorithm," in *2019 14th IEEE International Conference on Electronic Measurement & Instruments (ICEMI)*, 1020–1026, Changsha, China, 2019.

[33] Ye, F., J. Wang, Z. Li, Z. Jihan, and C. Yang, "Jane Street Stock prediction model based on LightGBM," in *2021 6th International Conference on Intelligent Computing and Signal Processing (ICSP)*, 385–388, Xi'an, China, 2021.

[34] Onoja, M., A. Jegede, J. Mazadu, G. Aimufua, A. Oyedele, and K. Olibodum, "Exploring the effectiveness and efficiency of LightGBM algorithm for windows malware detection," in *2022 5th Information Technology for Education and Development (ITED)*, 1–6, Abuja, Nigeria, 2022.

[35] Zhu, Y.-g. and Y.-f. Zhu, "Robust temporal constraint optimization based on Bayesian optimization algorithm," in *2010 International Conference on Computational and Information Sciences*, 186–189, Chengdu, China, 2010.

[36] Long, Y. and S. Huang, "Application of bayesian optimization in router port testing: An improved port scanning technique," in *2023 IEEE 5th International Conference on Power, Intelligent Computing and Systems (ICPICS)*, 98–103, Shenyang, China, 2023.

[37] Wang, M., Y. Zhu, H. Li, J. Zhou, and P. Wang, "Bayesian optimization for antenna design via multi-point active learning," in *2020 IEEE MTT-S International Conference on Numerical Electromagnetic and Multiphysics Modeling and Optimization (NEMO)*, 1–3, Hangzhou, China, 2020.

[38] Cui, L., Y. Zhang, R. Zhang, and Q. H. Liu, "A modified efficient KNN method for antenna optimization and design," *IEEE Transactions on Antennas and Propagation*, Vol. 68, No. 10, 6858–6866, 2020.

[39] Vedipala, V. R., A. R. Radharapu, A. K. Gajula, S. Sivani, and A. Akshaya, "U-slot loaded half-circled microstrip patch antenna

analysis using XGBOOST machine learning algorithm," in *2023 8th International Conference on Communication and Electronics Systems (ICCES)*, 804–809, Coimbatore, India, Jun. 2023.

[40] Harkare, A. H., N. C. Kakde, P. V. Pandit, N. R. Dhakate, A. G. Kothari, and A. A. Bhurane, "Design and optimization of rectangular dielectric resonator antenna for C-band frequencies using machine learning techniques," in *2024 IEEE Microwaves, Antennas, and Propagation Conference (MAPCON)*, 1–4, Hyderabad, India, Dec. 2024.